Charmonium with three flavors of dynamical quarks[*]

Massimo di Pierro[a], Aida X. El-Khadra[ab], Steven Gottlieb[ac], Andreas S. Kronfeld[a], Paul B. Mackenzie[a], Damian P. Menscher[b], Mehmet B. Oktay[b], and James N. Simone[a]

[a] Fermi National Accelerator Laboratory, P.O. Box 500, Batavia, IL 60510

[b] Department of Physics, University of Illinois, Urbana, IL 61801

[c] Department of Physics, Indiana University, Bloomington, IN 47405

We present a calculation of the charmonium spectrum with three flavors of dynamical staggered quarks from gauge configurations that were generated by the MILC collaboration. We use the Fermilab action for the valence charm quarks. Our calculation of the spin-averaged 1P–1S and 2S–1S splittings yields a determination of the strong coupling, with $\alpha_{\overline{\mathrm{MS}}}(M_Z) = 0.119(4)$.

1. INTRODUCTION

The current experimental program of precision flavor physics at the B factories, at CESR-c, and at the Tevatron needs accurate lattice QCD calculations of the relevant hadronic matrix elements to yield stringent constraints on the CKM sector of the standard model. Precision lattice QCD results in turn require that the systematic errors associated with lattice calculations be brought under control to the desired accuracy. The most important sources of systematic error in lattice calculations include the incomplete inclusion of sea quarks (quenched approximation), lattice spacing artifacts, perturbative errors, and the chiral extrapolation. We are planning a series of lattice calculations of the phenomenologically most important quantities in the B, D, $\bar{c}c$ and $\bar{b}b$ systems. We will address the first two sources of systematic error by performing simulations with highly improved actions on gauge configurations with $n_f = 2 + 1$ improved staggered quarks [1]. This effort must be complemented by the corresponding perturbative matching calculations of the improvement coefficients and currrent renormalizations. This should be possible with recent advances in automated perturbation theory [2].

The MILC collaboration has generated dynamical gauge configurations [3] using improved staggered and gluon actions. Their configurations include three (or $2 + 1$) flavors of light staggered fermions at several different light quark masses ranging from m_s to $m_s/5$. Hence, the systematic errors usually associated with the quenched approximation should be absent with these configurations. Furthermore, since numerical simulations with rather light quark masses are feasible with staggered actions, the issue of chiral extrapolations may be carefully studied.

The heavy quark action used in this work is based on Ref. [4]. It is related to NRQCD, but uses the four component fields and operators of the Wilson action rather than the two component fields and operators of NRQCD. Similar to NRQCD, the space-like and time-like components of the operators are uncoupled, and the coefficients of the operators are mass dependent. This action smoothly interpolates between an ordinary light quark action as $am \to 0$ and NRQCD when $am > 1$, but is applicable at all values of am. Our formalism can be regarded as a summation of terms of the form $(am)^p$ to all orders in the normalizations of operators, which is useful when $m \gg \Lambda_{\mathrm{QCD}}$. To $O(a)$, our action uses the same operators as the clover action [5]. Starting at $O(a^2)$, the operators are somewhat differ-

ent from those in the analogous light quark action. The reason is that a two-hop correction to the Wilson time derivative operator cannot be used because it introduces ghost states for heavy quarks. Its effects must instead be duplicated with Hamiltonian-style operators [6]. The action may be particularly useful for the charm quark on lattice spacings with $am_c < 1$. It has smaller discretization errors than standard light quark actions since the $(am_c)^p$ errors, which it resums and eliminates, are much larger than the remaining $(a\Lambda_{\mathrm{QCD}})^p$ discretization errors. Since it has a well-defined $a \to 0$ limit, it may be more convergent for $am < 1$ than NRQCD, which does not.

Now that we are calculating with dynamical quarks, lattice spacings obtained from the simplest quantities should all agree within errors. We start our work with a study of the charmonium spectrum, to test our methods and lattices. As a byproduct, we obtain a new determination of the strong coupling.

2. DETAILS OF THE CALCULATION

MILC uses the Asqtad action [3] for the staggered fermions which contains errors of $O(\alpha_s a^2)$, and an improved gluon action with $O(\alpha_s^2 a^2)$ errors. For the charm quarks we use the Sheikholeslami-Wohlert action [5] (which has $O(\alpha_s a)$ errors) with the Fermilab interpretation [4]. The quenched gauge configurations are generated with the Wilson gauge action. Table 1 lists the simulation parameters for all three lattices. The quenched lattice has a slightly smaller lattice spacing than the MILC lattices.

As usual, we calculate charmonium two-point functions using smeared source and sink operators. For this purpose, when working on MILC lattices, we use the Richardson potential [7] model wave functions shown in Figure 1. The quenched propagators were generated using Coulomb wave functions.

2.1. Fits

As shown in Refs. [8,9], constrained fits allow for better control of the systematic error due to excited state contributions, because they allow us

Table 1
Simulation parameters for the three lattices.

Size	$16^3 \times 32$	$20^3 \times 64$	$20^3 \times 64$
n_f	0	3	$2+1$
β	5.9	6.85	6.76
configs	300	174	298
am_s	∞	0.05	0.05
am_l	∞	0.05	0.01
κ_{ch}	0.1227	0.113	0.113
wf's	δ, 1S, 2S	δ, 1S	δ, 1S

to fit the correlators to a large number of states without loss of accuracy. Furthermore, with constrained fits one is also able to use all of the time slices in the fits without adjusting $t_{\min}$ and $t_{\max}$ to determine the best fit. We investigate this issue by comparing constrained and unconstrained fits. We fit meson correlators to the form

$$G(t; \{Z_n\}, \{E_n\}) = \tag{1}$$
$$\sum_n Z_n^2 (e^{-E_n t} + e^{-E_n(T-t)}).$$

We force our energy levels to be ordered by defining

$$\Delta E_n = E_n - E_{n-1} \equiv \exp(\epsilon_n). \tag{2}$$

In our fits we use Baysian statistics,

$$\chi^2 \to \chi^2_{\mathrm{aug}} \equiv \chi^2 + \chi^2_{\mathrm{prior}}, \tag{3}$$

where χ^2_{prior} is used to constrain E_0, ϵ_n, and Z_n to a predetermined range.

For simplicity, we test our fit program on the quenched lattice. Figures 2–3 show our fit results for the η_c ground and first excited state energies as functions of the number of states in the fit (n) obtained from the η_c propagator with a δ-function source and sink. We observe that the fit results — particularly the error bars — for the ground and first excited state energies are stable under adding more states to the fit when constrained fits are used, but not in the case of unconstrained fits. The unconstrained fits do not use Eq. 3, but they do use the energy ordering constraint of Eq. 2, which is probably the reason for the relative stability of the central fit values even in the unconstrained case.
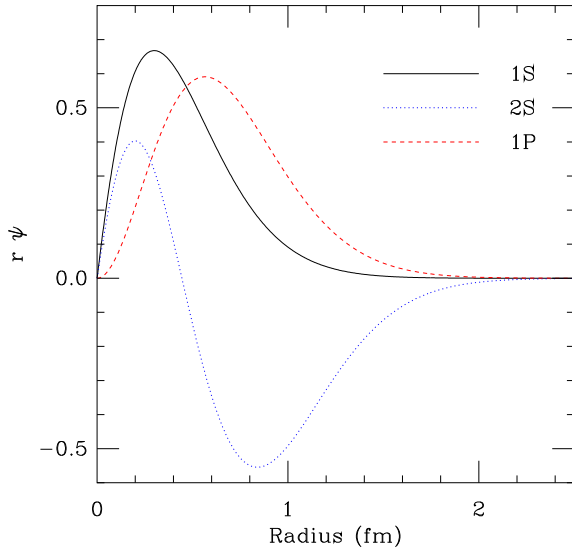
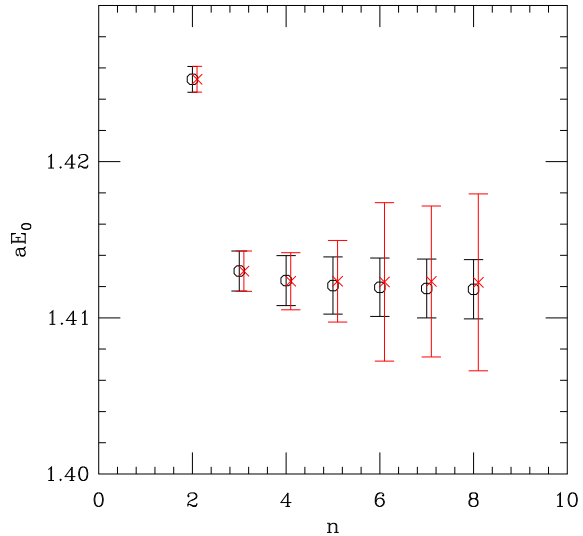Figure 1. Wavefunctions for the $1S$, $2S$, and $1P$ states in charmonium.

Figure 2. Comparison of fit results from constrained and unconstrained fits. Shown is the η_c ground state energy—obtained from the local-local correlator as a function of the number of states in the fit (n). ∘: constrained fit, ×: unconstrained fit

The prior constraints must be chosen so that they do not unduly influence the physical results. Figure 4 shows the dependence of the ground state fit on the prior width. The fit includes four states and the ranges for all priors are varied together with the ground state energy prior width. We see that the fit results are stable, once the prior width is large enough. Furthermore, the error on the ground state energy is unaffected by the variation of the prior width, after the plateau is reached. Table 2 lists typical choices for the energy prior values and ranges used in our fits. The prior values for the Z_n are chosen by match-

Table 2
Typical energy prior values and ranges.

n_f	0	3	$2+1$
η_c: E_0	1.4 ± 0.2	1.9 ± 0.2	1.9 ± 0.2
ΔE_n	0.4 ± 0.2	0.4 ± 0.2	0.4 ± 0.2
h_c: E_0	1.7 ± 0.2	2.3 ± 0.2	2.3 ± 0.2
ΔE_n	0.4 ± 0.2	0.5 ± 0.2	0.4 ± 0.2

ing the hadron propagators evaluated at $t = 1$ to Eq. 1; the range is usually set to a factor of three of the central value.

The results discussed in the next section are obtained from fits to multiple correlators, making use of the different source and sink operators listed in Table 1. These fits are generally consistent with fits to the delta-function correlators, albeit with smaller statistical errors.

3. THE SPECTRUM

Figure 5 summarizes our results for the charmonium spectrum. Our results for the hyperfine, 1P–1S, and 2S–1S splittings are shown in Figures 6–8 as functions of the light quark mass. We observe very little light quark mass dependence in the hyperfine splitting, and our chirally extrapolated result still disagrees with experiment, although the inclusion of dynamical quarks has removed one possible cause of a small hyperfine
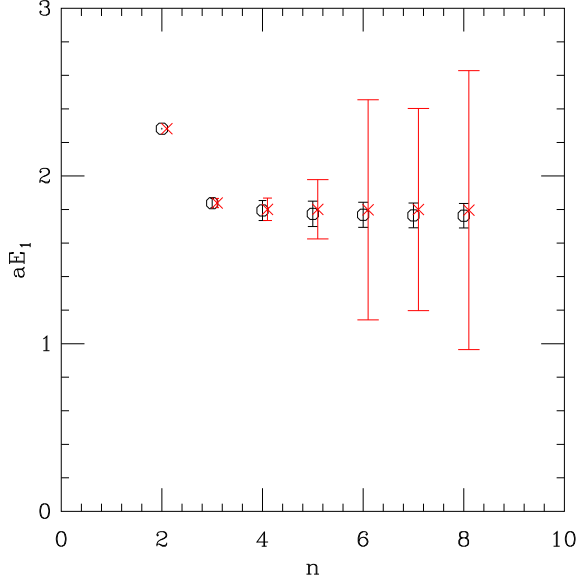
Figure 3. Same as Figure 2, but for the first excited state, the η_c'.

Figure 4. Variation of the η_c ground state energy fit result with the prior width. i is defined via $\sigma = 2^i\sigma_0$, where σ and σ_0 are the varied and standard choice of prior widths respectively.

splitting: the fact that the short distance coupling constant is too small in the quenched approximation. We note that the charm quark action is only $O(a)$ improved. The leading order operator which controls the spin splitting is $\bar{\psi}\sigma_{\mu\nu}F_{\mu\nu}\psi$. Its coefficient is being included only at tadpole improved tree-level, and it is plausible that the observed discrepancy is a result of both $O(\alpha_s a)$ errors and $O(a^2)$ lattice spacing artifacts. We will be able to study this issue further once our $O(a^2)$ improved action [6] is ready for numerical simulations.

The spin-averaged 1P–1S and 2S–1S splittings are considerably less sensitive to the leading order lattice artifacts; they are used to determine the lattice spacing. Figures 7–8 indicate that the dependence of the spin-averaged splittings on the light quark mass is mild.

The extent to which the lattice spacings from the 1P–1S and 2S–1S splittings disagree with each other is an indication of residual systematic errors in our simulation, which are a combination of higher order lattice spacing and sea quark effects. For this comparison we compute the ratio
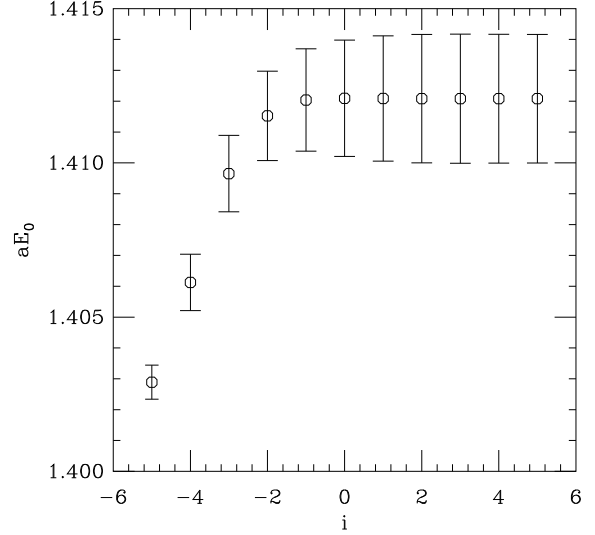
of lattice spacings,

$$R \equiv \frac{\frac{\Delta M(2S-1S)}{\Delta M(1P-1S)}^{\text{lat}}}{\frac{\Delta M(2S-1S)}{\Delta M(1P-1S)}^{\text{exp}}} \qquad (4)$$

Table 3 compares the lattice spacings obtained on all three lattices. On the quenched lattice the deviation of R from unity is about 1.5 standard deviations. On the two MILC lattices, the deviation of R from unity is less significant, because of the still somewhat large statistical errors. To

Table 3
The lattice spacings from the spin-averaged 1P–1S and 2S–1S splittings for the three lattices with statistical error bars.

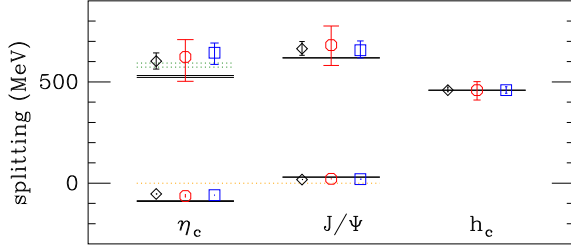| n_f	a^{-1}(1P–1S) (GeV)	a^{-1}(2S–1S) (GeV)	R
0	$1.783^{+0.062}_{-0.030}$	$1.637^{+0.079}_{-0.059}$	$1.089^{+0.057}_{-0.052}$
3	$1.70^{+0.16}_{-0.18}$	$1.52^{+0.15}_{-0.11}$	$1.12^{+0.14}_{-0.17}$
$2+1$	$1.564^{+0.058}_{-0.053}$	$1.426^{+0.073}_{-0.070}$	$1.097^{+0.073}_{-0.068}$

Figure 5. The charmonium spectrum in comparison. $\diamond$: $n_f = 0$, $\circ$: $n_f = 3$, $\square$: $n_f = 2 + 1$.
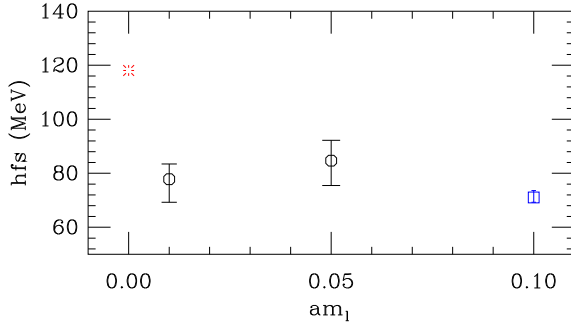

Figure 6. The hyperfine splitting *vs.* am_l (circles)). Shown also is the quenched result (square), positioned in the plot at finite am_l for illustration, and the experimental result (burst) positioned at $am_l = 0$.

Figure 7. The 1P–1S splitting *vs.* am_l (circles). Shown also is the quenched result (square), positioned in the plot at finite am_l for illustration.

Figure 8. The 2S–1S splitting *vs.* am_l (circles). Shown also is the quenched result (square), positioned in the plot at finite am_l for illustration.

clarify the situation we need to reduce the statistical errors of the results on the MILC lattices.

Now that dynamical fermions are included in the calculations, lattice spacings from the best-understood quantities should be consistent. We note that although the lattice spacings obtained from the 1P–1S and the 2S–1S splittings are consistent with each other, the lattice spacing from the 1P–1S splitting is consistent with several determinations of the lattice spacing from the Υ system [10], while the one obtained from the 2S–1S splitting is not. It is possible that higher order discretization effects are responsible for this.
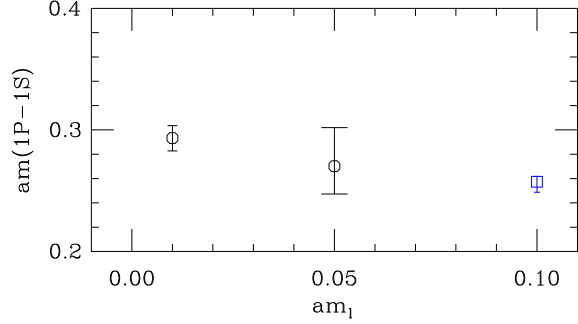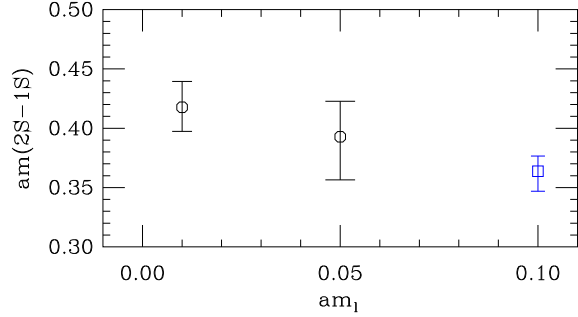
A more interesting possibility is that due to the fact that the 2S is so close to the $D\overline{D}$ threshold, physical effects from the coupling to $D\overline{D}$ channels may have a more dramatic effect in the 2S than in other states.

4. THE STRONG COUPLING

The spin-averaged splittings discussed in the previous section are used to determine the strong coupling α_s. The $2 + 1$ flavor lattices are our most realistic. We take the 1P–1S splitting as our

most reliable determination of the lattice spacing because of the possible threshold effects in the 2S state. Following the procedure of Ref. [11], we obtain the strong coupling from the plaquette. For our actions we have [12]

$$-\ln\langle\text{Tr}\,U_P\rangle = \qquad\qquad (5)$$
$$3.0682\,\alpha_P(q^*)\left[1 - \alpha_P(0.770 + 0.09681\,n_f)\right]$$

where $q^* = 3.33/a$ is the BLM scale for $n_f = 3$. The coupling α_P is defined to coincide through one-loop order with α_V, the coupling defined from the heavy quark potential. Using

$$\alpha_{\overline{\text{MS}}}(q) = \alpha_P\left(e^{5/6}\,q\right)\left[1 + \frac{2}{\pi}\alpha_P + O(\alpha_P^2)\right], \quad (6)$$

we obtain

$$\alpha_{\overline{\text{MS}}}(M_Z) = 0.119 \pm 0.004. \qquad (7)$$

The difference between our value and the value reported in Ref. [12] arises mainly from differing implicit treatment of $O(\alpha^3)$ corrections, which will soon be known. The main sources of uncertainty are $O(\alpha^3)$ corrections (3%), discretization errors (2%), and statistical errors (1%). All three should be significantly reduced soon.

5. CONCLUSIONS AND OUTLOOK

We present preliminary results of a calculation of the charmonium spectrum on gauge configurations generated by the MILC collaboration using $O(a^2)$ improved actions for the gluons and the $n_f = 2 + 1$ dynamical staggered fermions. We use the $O(a)$ improved clover action with the Fermilab interpretation for the charm valence quarks. Since the MILC configurations were generated with the correct number of sea quarks, no extrapolation in n_f is necessary. Furthermore, the nondegenerate strange and light quark masses in the MILC lattices allow us to consider the chiral limit. Comparing results at $am_s = am_l = 0.05$ and $am_s = 0.05, am_l = 0.01$, we find only mild light quark mass dependence for all spectral quantities we consider. Finally, our calculation yields a new determination of the strong coupling where systematic errors due to sea quark effects are under control.

For future work, we are planning to improve the statistical accuracy of this work. The improvement of the heavy quark action beyond $O(a)$ is in progress [6].

REFERENCES

1. T. Blum et al., Phys. Rev. D55 (1997) R1133; J. Lagae and D. Sinclair, Phys. Rev. D59, (1998) 104511; G. P. Lepage, Phys. Rev. D59 (1999) 074502; K. Orginos, D. Toussaint, and R. Sugar, Phys. Rev. D60 (1999) 054503; C. Bernard et al., Phys. Rev. D61 (2000) 111502(R).
2. M. Nobes and H. Trottier, these proceedings, hep-lat/0209017.
3. C. Bernard et al.(MILC collaboration), Phys. Rev. D64 (2001) 054506.
4. A. El-Khadra, A. Kronfeld and P. Mackenzie, Phys. Rev. D55 (1997) 3933.
5. B. Sheikholeslami and R. Wohlert, Nucl. Phys. B259 (1985) 572.
6. M. B. Oktay et al., these proceedings, hep-lat/0209150.
7. J.L. Richardson, Phys. Lett. B82 (1979) 272.
8. G.P. Lepage et al., Nucl. Phys. Proc. Suppl. 106 (2002) 12.
9. C. Morningstar, Nucl. Phys. Proc. Suppl. 109 (2002) 185.
10. A. Gray et al., these proceedings, hep-lat/0209022.
11. P. Lepage and P. Mackenzie, Phys. Rev. D48 (1993) 2250.
12. C. Davies et al., these proceedings, hep-lat/0209122.